

1 **Interaction between East Asian summer monsoon and westlies as**
2 **shown by tree-ring records**

3

4 Xiao Shengchun^{1*}, Peng Xiaomei¹, Tian Quanyan¹, Ding Aijun², Xie Jiali¹, Su
5 Jingrong^{1,3}

6

7 ¹ Key Laboratory of Ecological Safety and Sustainable Development in Arid Lands,
8 Northwest Institute of Eco-Environment and Resources, Chinese Academy of
9 Sciences, Lanzhou, Gansu, China 730000.

10 ² College of Resources and Environment, Gansu Agricultural University, Lanzhou,
11 Gansu, China 730070.

12 ³ University of Chinese Academy of Sciences, Beijing, China 100049.

13 * Corresponding author (xiaosc@lzb.ac.cn).

14 Address: 320 West Donggang Road, Lanzhou City, Gansu Province, China.

15 Zip Code: 730000.

16

17 **Abstract:**

18 Atmospheric circulation changes, their driving mechanisms and interactions are
19 important topics in global change research. Local changes in the East Asian summer
20 monsoon (EASM) and the mid-latitude westerlies will inevitably affect the climate and
21 ecology of the arid zone of Northwest China. Hence, it is important to study these
22 regional changes. While previous studies in this area are all single-point climate
23 reconstruction studies, there is a lack of research on the interaction areas and driving
24 mechanisms of the two major circulations. Dendroclimatology can provide high-
25 resolution, long-term, and reliable multi-point proxies for the study of inter-annual and
26 inter-decadal climate change. We chose to observe these changes in the Alxa Plateau
27 using dendrochronological methods. We assembled ring-width records of Qinghai
28 spruce (*Picea crassifolia*) in the mountain regions surrounding the Alxa Plateau: the
29 Helan Mountains, Changling Mountain, and Dongdashan Mountain. The results show
30 that radial growth was indeed affected by changes in the monsoon and westerlies. The
31 heterogeneity of precipitation and climatic wet-dry changes in different regions is
32 primarily influenced by the interactions between atmospheric circulation systems, each
33 with its own dominant controlling factors. In the case of the Helan Mountains, both of
34 these major atmospheric circulation systems play a significant role in shaping climate
35 changes. Changling Mountain in the southern part of the Alxa Plateau is mainly
36 influenced by the EASM. Dongdashan Mountain is mainly influenced by the westerlies.
37 Understanding these local conditions will help us predict climate changes in Northwest
38 China.

39

40 **Key words:** Alxa Plateau, dendroclimatology, westerlies, EASM, interaction between
41 winds and monsoon.

42

43 **1. Introduction**

44 The alpine zone of Qinghai-Tibet, the arid zone of the northwestern interior, and
45 the humid zone of the east constitute the three main areas of China's natural
46 geomorphology (Chen et al., 2019a). The Northwest China inland dry zone is located
47 in the hinterland of the Eurasian continent and is among the driest regions in the world.
48 It displays typical climatic characteristics of a continental climate. This region is mainly
49 influenced by the westerlies and the ~~EASM~~ (the East Asian summer monsoon (EASM)).
50 The interaction of these two factors results in high precipitation variability and hence
51 frequent droughts. This was true even before the onset of global climate change in the
52 area, and it is even more pronounced in recent years. This inland arid zone is
53 ecologically fragile (Chen et al., 2019a; Chen et al., 2019b; Zhang et al., 2023).

54 The semi-arid and arid regions of northern China are characterized by large areas
55 of sand and desert. They are the second largest source of dust in the world after the
56 Sahara. Their contribution to global climate change is large. So far inland, the influence
57 of the EASM is often weak (Zhang et al., 2021; Liu et al., 2022). It is opposed by the
58 westerlies that flow from the North Atlantic climate zone toward the East Asian
59 monsoon climate zone (Qu et al., 2004). The interaction between the westerlies and the
60 EASM governs precipitation, water vapor transport, and thus the climate of
61 northwestern China (Feng et al., 2004; Wang et al., 2005; Li et al., 2008; Ma et al.,
62 2011).

63 To estimate the impact of global change on this interaction, it is crucial to
64 comprehend its historical context. Global atmospheric circulation is likely to change,
65 as is the EASM. Climate change will not only affect the regional climate and regional
66 water resources (Ding et al., 2023); it will affect East Asia (dust storms) and even the
67 rest of the globe. Hence, the study of climate in this region is of great practical and
68 theoretical significance (Chen et al., 2019a; Chen et al., 2019b).

69 The westerlies and the EASM meet at the northern boundary of the Asian summer
70 monsoon (Huang et al., 2023). In northern China, this boundary runs from west to east,
71 along the eastern section of the Qilian Mountains, the southern foothills of the Helan
72 Mountains, the Daqing Mountains, and the western section of the Daxinganling

73 Mountains. This is not a static boundary. It fluctuates within a range of 200–700 km
74 (Chen et al., 2018). It is important to understand the history of these fluctuations (Huang
75 et al., 2023).

76 This can be done using climate records such as lacustrine, eolian, and
77 dendrochronological (Sun et al., 2003; Liu et al., 2005; Li, 2009; Chen et al., 2010; Li
78 et al., 2016; Chen et al., 2019b; Qin et al., 2023). Dendrochronology is one of the best
79 tools for studying paleoclimatic changes, due to its precise dating, high resolution, good
80 continuity and high replication (Zhang et al., 2003; Shao et al., 2010; Yang et al., 2014;
81 Liu et al., 2016).

82 The climate history of the Baotou area, at the northern edge of the EASM, has been
83 studied at interannual and interdecadal scales for the past 260 years, based on June–
84 August precipitation reconstruction from tree-ring samples from the western Yinshan
85 Mountains (Liu et al., 2001; Liu et al., 2003). Using tree-rings and historical records,
86 Kang and Yang (2015) reconstructed the annual precipitation history of the East Asian
87 monsoon northern fringe zone for the last 530 years. They analyzed spatial variability
88 and possible driving mechanisms using the 400-mm isohyet.

89 Several May–July precipitation sequences have been reconstructed using ring-
90 width and latewood-width data from Chinese pine (*Pinus tabulaeformis*) growing in
91 the Helan Mountains (Ma et al., 2003; Liu et al., 2004; Chen et al., 2016). Studies of
92 tree-ring carbon and oxygen isotopes from Chinese pine samples have shown that $\delta^{18}\text{O}$
93 values increase with summer precipitation, while $\delta^{13}\text{C}$ values decrease (Zhang et al.,
94 2005a; Liu et al., 2008). westerlies have also been shown to affect precipitation in the
95 Helan Mountains (Chen et al., 2010).

96 Principal component analysis of tree-ring chronologies constructed from data
97 collected at several sites in Gansu suggests that trees at these sites were more influenced
98 by EASM than by westerlies (Chen et al., 2013). These researchers also found that the
99 EASM weakened in 1970s, but recovered in the early 1990s. Tree-ring data allowed the
100 reconstruction of 330 years of PDSI (Palmer Drought Severity Index) values for the
101 Mount Hasi region (at the northern boundary of the summer monsoon zone) (Kang et
102 al., 2012). This study confirmed that radial growth of Chinese pine has declined over

103 the past three decades, due to the weakening of the EASM. Dendrochronological
104 reconstruction of precipitation in the Mount Changling region (again using Chinese
105 pine) suggested that precipitation in that region mainly depends on the EASM (Chen et
106 al. 2012). Other researchers have assembled tree-ring chronologies from pines growing
107 in the Mount Qilian region and the northern mountains of the Hexi Corridor. Here again
108 precipitation is associated with the EASM. These chronologies have allowed scholars
109 to compile precipitation, temperature, and drought records for the last thousand years
110 (Gou et al., 2015a; Gou et al., 2015b; Zhang et al., 2017).

111 Most modern researchers studying climate change in the region are mostly carried
112 out on single sample sites (Wang et al., 2004; Liu et al., 2005; Chen et al., 2010; Chen
113 et al., 2016; Li et al., 2016; Liu et al., 2016; Chen et al., 2018). While, there is a dearth
114 of multi-site, regional and long time scale studies on the interaction of the westerlies
115 and the EASM. The research focuses on the interplay area, and investigates the
116 spatiotemporal heterogeneity in climate change and its dominant driving factors,
117 specifically related to the westerlies and East Asia monsoon circulation in Alxa Plateau.

118 ~~Compiled and analyzed tree-ring chronologies from~~ Qinghai spruce (*Picea*
119 *crassifolia*) ~~growing is a common tree species~~ in the Helan, Changling, and Dongdasha
120 mountain ~~regions that surround areas around~~ the Alxa Plateau, ~~—~~. Using
121 dendrochronological methods, we analyzed the climate response characteristics of
122 spruce radial growth ~~in on the above three regions was then analyzed~~ mountains.
123 Combining the relevant Westerly and East Asia monsoon circulation indices, the
124 driving mechanism of the regional climate change by with the interaction and
125 synergistic roles of two atmospheric circulation systems in the Alxa Plateau was
126 explored. The results will lay a theoretical foundation for the climatic evolution of the
127 region and the desertification control.

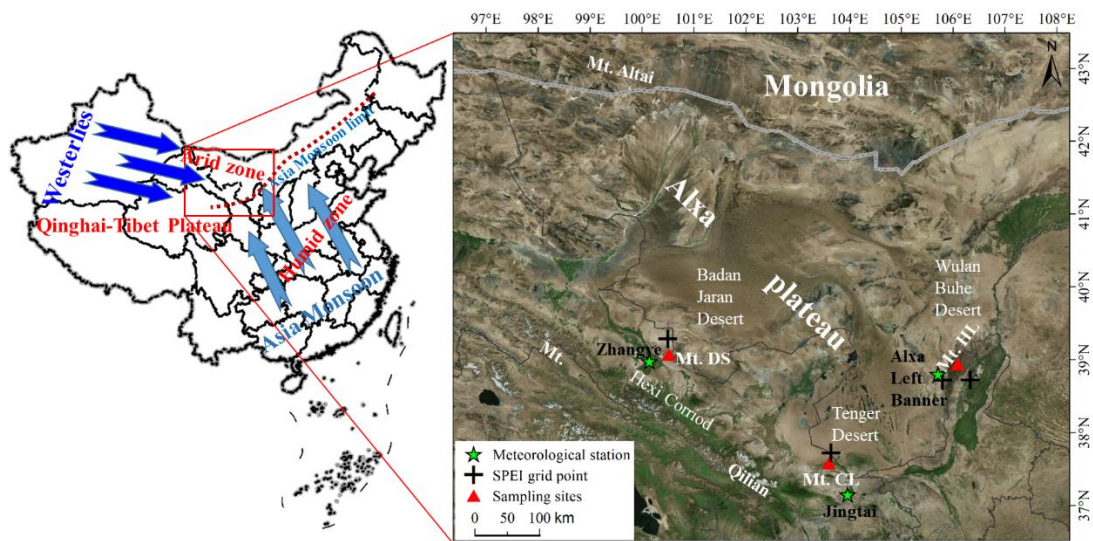
128

129 **2. Material and methods**

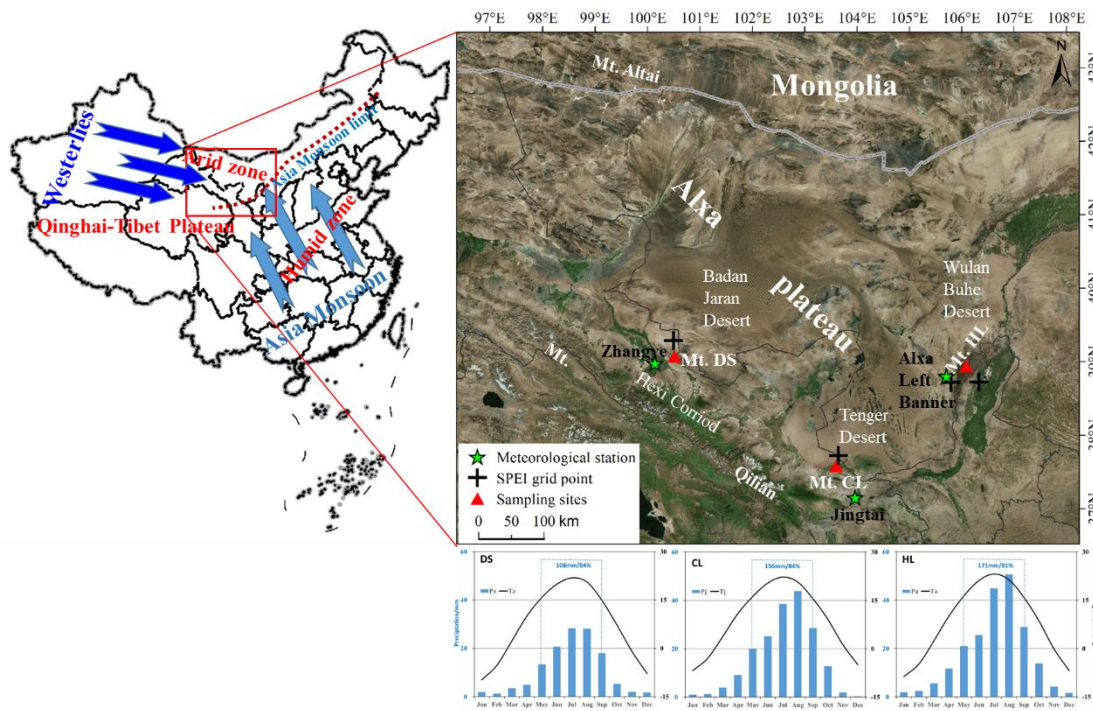
130 **2.1 Study area**

131 The Alxa Plateau is located in the western part of the Inner Mongolia Autonomous
132 Region and is surrounded by mountains (Fig.1). It consists primarily of three deserts:

133 Tengger, Ulan Buh, and Badan Jaran. It lies south of the Gobi desert. It is the main
 134 source of the fierce sandstorms and dust storms that blow toward eastern China and the
 135 Pacific. It has been much affected by climate change; sand- and dust storms have
 136 increased, much to the detriment of lands to the east. The Chinese government is doing
 137 what it can to establish an environmental defense line there. It is currently the Northern
 138 Sand Prevention Belt of the National Two Ecological Barrier and Three Belts
 139 Ecological Security Strategy Pattern (Xiao et al., 2017; Xiao et al., 2019).



140
 141 **Figure 1. Location of tree-ring sampling sites and meteorological stations (the right**
 142 **panel is from Mapworld).**



143

144 Figure 1. Location of tree-ring sampling sites and climatic diagram of study area. Pa/Ta are the
145 monthly total precipitation and monthly mean temperature at the Alxa Left Banner meteorological
146 station (1953–2016); Pj/Tj are the precipitation and temperature figures for the Jingtai
147 meteorological station (1957–2017); Pz/Tz are the precipitation and temperature figures for the
148 Zhangye meteorological station (1957–2017). The dashed box and appended data indicate the total
149 growing season precipitation in the study area and the proportion of total annual precipitation.

150
151 There are several mountain ranges surrounding the Alxa Desert, such as the Helan
152 Mountains in the east, the northern mountains of the Hexi Corridor, and the outliers of
153 the Altai Mountains in the north. These mountains not only block the eastward and
154 southward expansion of the desert (driven by high pressure regions from Mongolia);
155 they are also the source of mountain rivers and streams that water the oases on the
156 plateau.

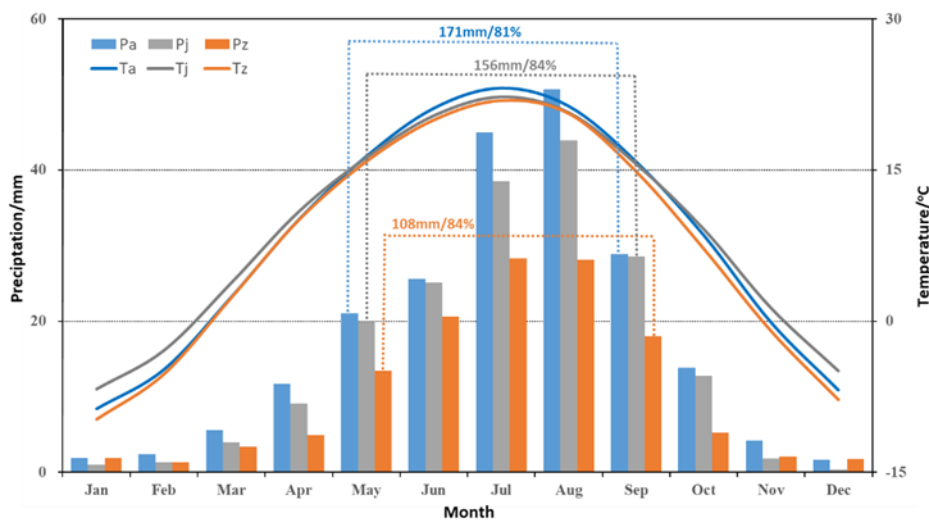
157 The Alxa Plateau is located in the eastern margin of the inland arid region of Central
158 Asia. It is affected not only by the mid-latitude westerly circulation, but also by the
159 Asian monsoon and the Tibet plateau monsoon. It is in the zone where the mid-latitude
160 westerly circulation and the Asian monsoon interact (Xiao et al., 2017; Chen et al.,
161 2019b). As a result, vegetation cover in this region there is largecharacterized by
162 pronounced interannual variability ~~of vegetation cover in the region~~ (Ou and Qian, 2006;
163 Tang et al., 2006; Li et al., 2013).

164 The Helan Mountains (38°27'~ 39°30'N, 105°20'~106°41'E) (sampling site
165 henceforth abbreviated as HL), are located at the eastern edge of the Tengger Desert.
166 They stretch more than 200 kilometers from north to south; the main peak is ~3,556 m.
167 The mountain forests are dominated by Qinghai spruce and Chinese pine, juniper,
168 mountain aspen, and elm.

169 Mount Changling (37°12'~37°17', 102°45'~103°48'E) (sampling site henceforth
170 abbreviated as CL) is an independent mountain protruding northward from the
171 remnants of the eastern Qilian Mountains, it is located at the southern edge of the
172 Tengger Desert; its elevations range from 2100 to 2900 m. The dominant tree species
173 are Qinghai spruce and Chinese pine.

174 Mount Dongdashan (39°00'~39°04'N, 100°45'~100°51'E) (sampling site
 175 henceforth abbreviated as DS) is located at the southwestern edge of the Badan Jaran
 176 Desert and the middle part of Mount Qilian. It is one of the northern mountains along
 177 the Hexi Corridor; that range consists of mountains that vary from 2200 to 2637 m in
 178 elevation. Forests are dominated by Qinghai spruce and Qilian juniper. The distances
 179 between the CL and HL, CL and DS, and DS and HL sampling sites are approximately
 180 250 km, 310 km, and 450 km, respectively.

181 The temperatures of the coldest months recorded at meteorological stations in the
 182 Alxa Left Banner (a division of the Alxa League region), Jingtai (a county in Gansu),
 183 and Zhangye (a city in Gansu) all occurred in January, ranging from -9.8°C to -6.8°C.
 184 The hottest months at those stations were in July (21.9 °C to 23.1 °C). These
 185 meteorological stations are the closest stations to our three sampling sites- (Fig.1).



186 **Figure 2. Climatic diagram of study area.** Pa/Ta are the monthly total precipitation and
 187 monthly mean temperature at the Alxa Left Banner meteorological station (1953–2016); Pj/Tj are
 188 the precipitation and temperature figures for the Jingtai meteorological station (1957–2017); Pz/Tz
 189 are the precipitation and temperature figures for the Zhangye meteorological station (1957–2017).
 190 The dashed box and appended data indicate the total growing season precipitation in the study area
 191 and the proportion of total annual precipitation.

193 Precipitation measured at those stations varied widely. The multi-year average of
 194 total precipitation from May to September was 171 mm at Alxa Left Banner station,

195 156 mm at Jingtai station, and 108 mm at Zhangye station. This accounted for more
196 than 80% of the annual precipitation (Fig.21).

198 **2.2 Sample collection, processing and data analysis method**

199 **2.2.1 Sample collection, processing and dendrochronology construction**

200 Researchers used standard methods of tree-ring sample collection. One core was drilled
201 from each tree in the sample site. We collected 209 cores in total, from five sampling
202 sites at HL, 48 cores from one sampling site at CL, and 81 cores from two sampling
203 sites at DS. Relevant information of the sampling sites is summarized in Table 1.

204 Chronologies were constructed using standard dendrochronological methods
205 (Cook, 1985). In order to highlight the high frequency signal, the RES chronology is
206 selected for later climate analysis. We calculated the highly significant correlations (P
207 < 0.001) between the chronologies of different points at the HL and DS mountains; a
208 weighting method was used to finally synthesize a chronology for each mountain.
209 Generally, the sub-sample signal strength (SSS) index and the mean series
210 intercorrelation (R_{bar}) are used to evaluate the credibility and quality of the chronologies.
211 The length of the reliable chronology is indicated by the parts of the series with a
212 subsample signal strength (SSS) index > 0.85 (Wigley et al., 1984). Another important
213 statistic is the mean series intercorrelation (R_{bar}), which is the mean correlation
214 coefficient among the ring series and is therefore an indication of the common variance.

216 **2.2.2 Climate data, atmospheric circulation indices and the related Analyzing 217 methods for chronological correlation**

218 Climate data for the study areas HL, CL, and DS were collected from the nearest
219 meteorological stations in Alxa Left Banner, Jingtai and Zhangye, respectively
220 (<http://data.cma.cn>).

221 We used SPEI (Standardized Precipitation Evapotranspiration Index) to represent
222 the local drought and wetness conditions, which is widely used in the dendrochronology
223 studies and considering the effects of potential evapotranspiration, precipitation and
224 time scales (Vicente-Serrano et al., 2010). SPEI data (grid-point resolution $0.5^{\circ} \times 0.5^{\circ}$)

225 was obtained from the grid-point datasets of the National Center for Environmental
226 Predictions-National Center for Atmospheric Research (NCEP-NCAR). Time scales
227 ranged from 1 month to 15 months. The mean values of data from two grid-points
228 closest to the HL sampling site (38.75°N, 105.75°E and 38.75°N, 106.25°E; period
229 1953–2015) were chosen for subsequent analysis. Grid-point data from one site closest
230 to our CL sampling site (37.75N, 103.75E; period 1951–2015) was used for later
231 analysis. Grid-point data from one site closest to our DS sampling site (39.25°N,
232 100.75°E; period 1951–2015) was also used. As SPEI datasets are multi-scale, we
233 preprocessed the data to identify and select 11-month scaled SPEI datasets for
234 subsequent analysis.

235 We took into account the so-called lagging effect (the influence of fall and winter
236 climate factors on the radial growth of trees shows up later in the year) and chose to use
237 temperature, precipitation, and SPEI data from September of the previous year to
238 September of the current year (abbreviated as P9–P12 and C1–C9), as collected at each
239 meteorological station, for our climate response analysis.

240 The East Asian Summer Monsoon Index (EASMI) (Li and Zeng 2005) represents
241 the activity strength of the EASM. Larger EASMI values indicate a stronger summer
242 monsoon, smaller ones a weaker monsoon. In this study, the EASMI (mean values for
243 June–August in the period 1950–2017) defined by Li and Zeng (2005) was used to
244 study the impact of the EASM on climate change in the study area.

245 The East Asian Summer Monsoon Index (EASMI) represents the activity strength
246 of the EASM. The East Asian summer monsoon (EASM) index is defined as an area-
247 averaged seasonally (JJA) dynamical normalized seasonality (DNS) at 850 hPa within
248 the East Asian monsoon domain (10°-40°N, 110°-140°E) (Li and Zeng 2005)。 Larger
249 EASMI values indicate a stronger summer monsoon, smaller ones a weaker monsoon.
250 In this study, the EASMI (mean values for June–August in the period 1950–2017)
251 defined by Li and Zeng (2005) was used to study the impact of the EASM on climate
252 change in the study area.

253 We used the Westerly Circulation Index (WCI annual mean; <https://cmdp.ncc->
 254 [cma.net/cn/index.htm](https://cmdp.ncc-cma.net/cn/index.htm)) to represent the strength of the mid-latitude westerlies. The
 255 larger the WCI value, the stronger the Eurasian latitudinal circulation; the smaller the
 256 value, the weaker the Eurasian latitudinal circulation. WCI data (period 1951–2015)
 257 were derived from the Eurasian Latitudinal Circulation Index published by the National
 258 Climate Center of the China Meteorological Administration (<https://cmdp.ncc->
 259 [cma.net/cn/index.htm](https://cmdp.ncc-cma.net/cn/index.htm)).

260 Interannual and interdecadal (sliding moving average of 11a) chrono-climatic/
 261 cyclonic index correlation and partial correlation analyses were performed using SPSS
 262 19.0. Based on the characteristics of tree-ring series, the sequences were classified into
 263 three groups of low, average and high ring widths using $\text{mean} \pm 1\delta$ (δ : standard
 264 deviation) as the classification criterion (with $\text{mean} \pm 2\delta$ as the extreme year).
 265 Correlation statistical tests were performed with the corresponding annual circulation
 266 indices; similar treatments and analyses were performed for the two major circulation
 267 indices.

268

269 **3. Results and analysis**

270 **3.1 Ring-width chronologies and their characteristics**

271 Based on the sampling cores from five sample sites at HL, two sample sites at DS, and
 272 one sample site at CL, ring-width residual chronologies were derived for each of the
 273 three study areas (Fig. 32). Statistical parameters showed that the three chronologies
 274 meet the usual requirements for correctly done dendrochronological studies (Table 1).

275 Table 1. Statistical characteristics of the sampling sites and the tree-ring chronologies.

276

277 Table 1. Statistical characteristics of the sampling sites and the tree-ring chronologies.

Sampling sites	HL(5)	CL(1)	DS(2)
Latitude (°N)	38.52–38.97	37.61	39.04
Longitude (°E)	105.83–106.02	103.71	100.78
Elevation (m)	2200–2750	2490	2650–2700
Cores	209	48	81

Reliable period	1891–2018	1866–2017	1823–2015
MS	0.18–0.37	0.28	0.15–0.33
R_{bar}	0.45–0.61	0.56	0.40–0.60
SNR	22.5–56.1	38.9	25.7–42.5
EPS	0.96–0.98	0.98	0.96–0.98
PC1(%)	17.3–63.0	57.9	43.0–62.5

278 Reliable period (SSS > 0.85), MS (mean sensitivity), R_{bar} (mean series intercorrelation), SNR (signal to
 279 noise ratio), EPS (expressed population signal), and PC1 (variance explained by the first principal
 280 component) refer to residual chronologies).

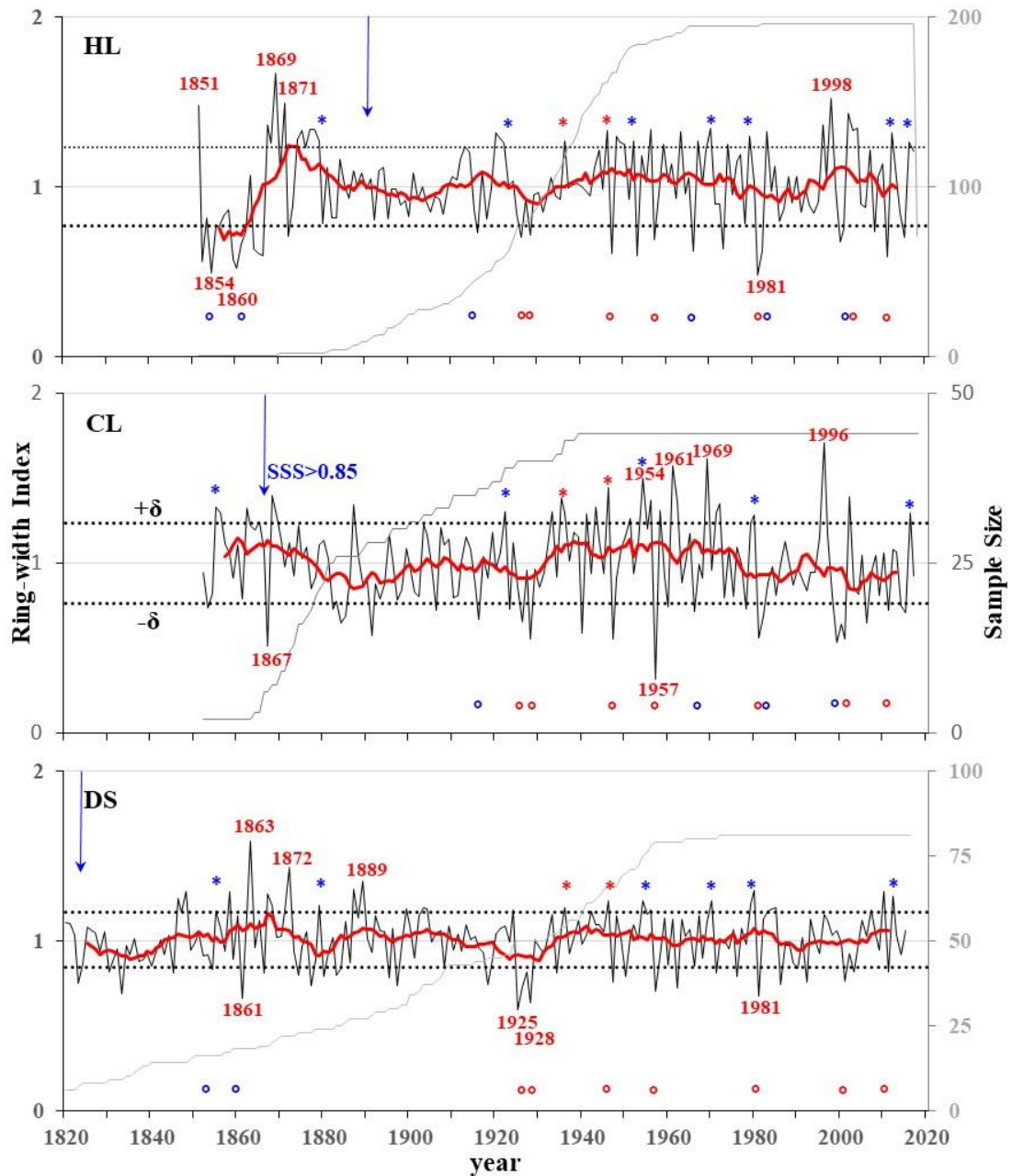
281

282 **3.2 Climate response characteristics**

283 Correlation analysis comparing a) monthly mean temperature and precipitation at
 284 neighboring meteorological stations and b) SPEI at the nearest grid-point showed that,
 285 overall, the three residual chronologies were correlated negatively with monthly mean
 286 air temperature, positively correlated with monthly precipitation, and positively
 287 correlated with SPEI during the growing season (Fig. 43).

288 HL chronology was correlated negatively with mean temperature mainly in C5–C8
 289 in the growing season, but not to the significant level. It was also positively correlated
 290 with precipitation in all months except P12, C1, and C9, reaching significant levels (P
 291 < 0.05) in P9, C5, and C6. All months were positively correlated with SPEI and reached
 292 statistical significance (P < 0.05), with C3–C8 showing highly significant correlation
 293 levels (P < 0.01).

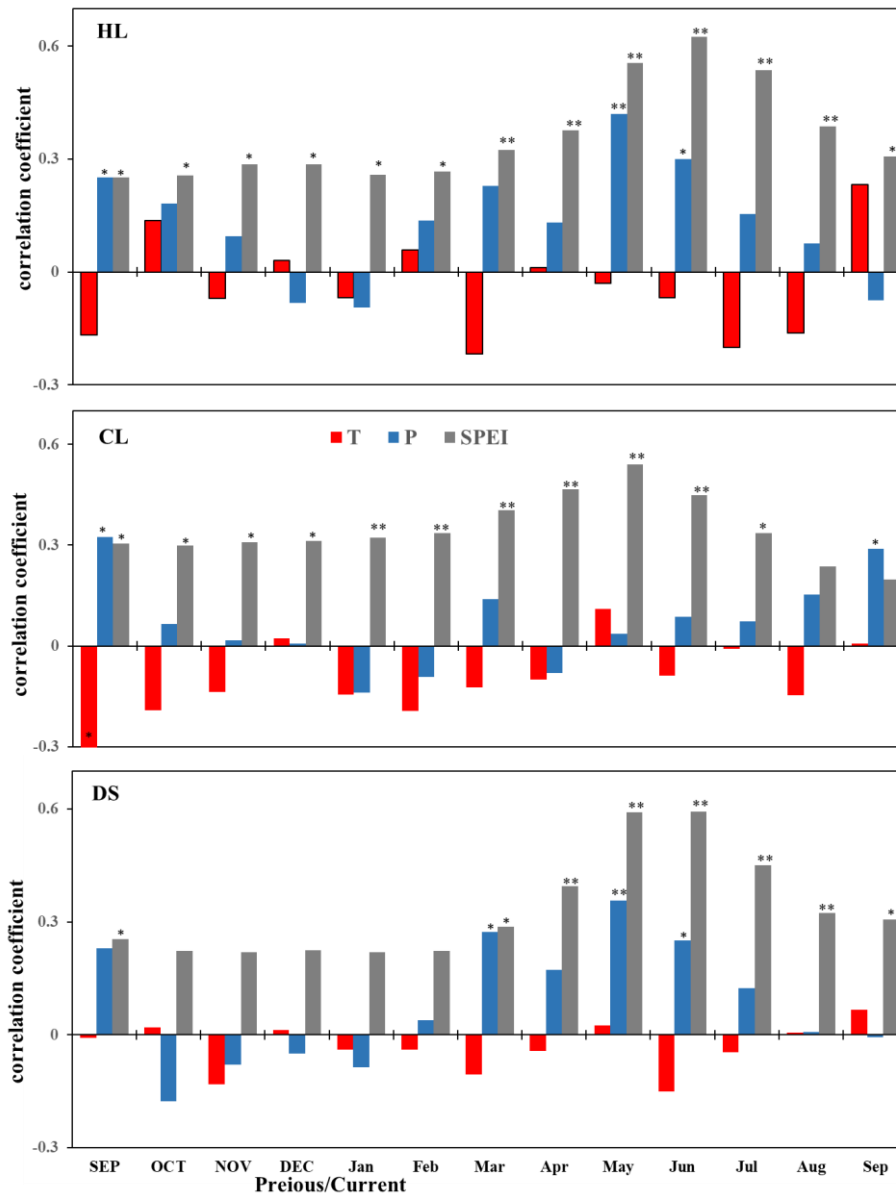
294



295

296 **Figure 32.** Residual ring-width chronologies for the three study areas. The dark lines indicate the
 297 chronology; grey lines indicate the sample depth; red lines indicate the 11-year running mean
 298 chronology; dotted horizontal lines indicate the mean value $\pm 1\delta$; years with data identified as $>/<$
 299 mean $\pm 2\delta$ (δ : standard deviation); blue * and o indicate the years shared between two of the three
 300 sample sites, red * and o shows years shared between three sample sites; blue arrows indicate the
 301 start of the reliable residual chronology ($SSS > 0.85$).

302



303

304 **Figure 43.** Correlation coefficients (Pearson's r values) between the residual ring-width
 305 chronologies of Qinghai spruce at the three study areas (HL, CL and DS) and the observed monthly
 306 temperature (T), total monthly precipitation (P), and SPEI. * Pearson's r correlation, significant at
 307 $P < 0.05$. ** Pearson's r correlation, significant at $P < 0.01$. Month names of previous year are
 308 capitalized.

309

310 CL chronology was negatively correlated with the mean temperature in most
 311 months, but only reached a significant negative correlation ($P < 0.05$) with P9. CL
 312 chronology was positively correlated with monthly precipitation, save for C1, C2, and
 313 C4. Only P9 and C9 reached statistical significance ($P < 0.05$). All months were

314 positively correlated with SPEI, with P9–C7 reaching significant correlation levels (P
315 < 0.05) and C1–C7 reaching highly significant correlation levels ($P < 0.01$).

316 DS chronology showed weak correlations between DS chronology and monthly
317 mean temperatures. None of the correlations reached levels of significance. DS
318 chronology was positively correlated with P9 and C2–C8 precipitation and reached
319 significant correlation levels for C3, C5, and C6 ($P < 0.05$). All months were positively
320 correlated with SPEI, with P9 and C3–C9 reaching significant correlation levels ($P <$
321 0.05) and C4–C8 reaching highly significant correlation levels ($P < 0.01$).

322 Overall, the radial growth of Qinghai spruce at the three study areas seems to have
323 been limited, for the most part, by low precipitation during the growing season (April–
324 July). The three chronologies reflect regional wet and dry variations.

325

326 **3.3 Regional climate changes as recorded by tree-ring widths**

327 **3.3.1 Regional climate change viewed at interannual scales**

328 On interannual scales, the three residual chronologies, when compare, showed highly
329 significant correlations (HL–CL: $n = 166$, $r = 0.298$, $P < 0.001$; HL–DS: $n=165$, $r=0.331$,
330 $P < 0.001$; CL–DS: $n = 164$, $r = 0.374$, $P < 0.001$). This indicates that there was a high
331 degree of consistency in the radial growth of Qinghai spruce in the three regions.

332 According to the results of the chronology-climate response analysis in the
333 previous section, the high and low ring-width indices ($\text{mean} \pm 1\sim 2\delta$) of the chronology
334 at the three sample sites indicate wetter or drier, and extreme wet or dry years,
335 respectively (Fig. 32).

336 Overall, the three ring-width residual chronologies (HL, CL, DS) had a total of two
337 shared wetter years and seven shared drier years. The HL and CL chronologies shared
338 four wet years and eleven dry years; the HL and DS chronologies shared five wet years
339 and nine dry years; and the CL and DS chronologies shared five wet years and seven
340 dry years (Fig. 32).

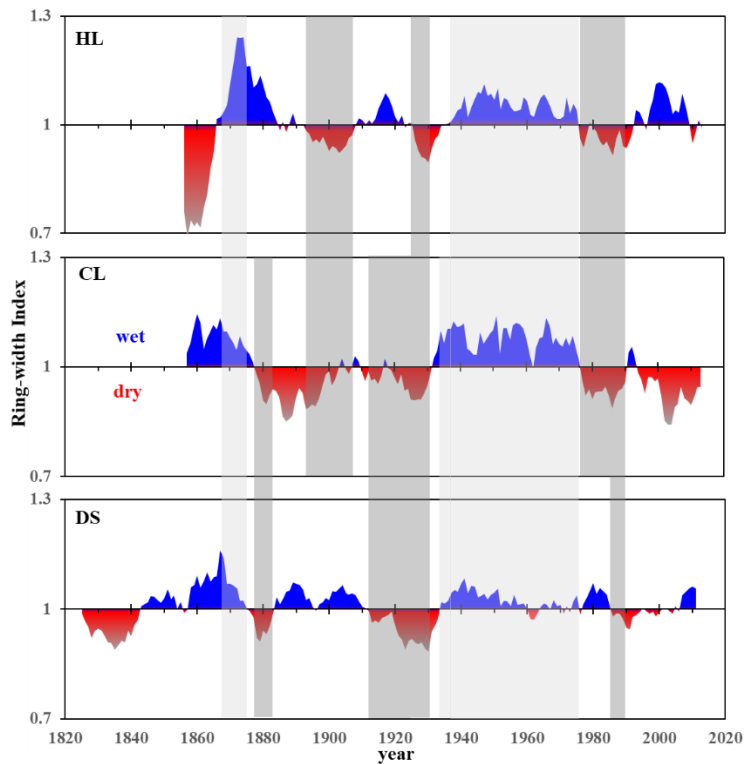
341 There were no extremely wet years shared by the three sample sites. However, there
342 were two shared wetter years in 1936 and 1946 and several shared wetter years in later
343 years among the three sample sites. For example, note the wetter years in 1922 and
344 2016 for HL and DS chronologies; 1959, 1979, and 2012 for HL and DS chronologies;
345 1855, 1954, and 1980 for CL and DS chronologies (Fig. 32).

346 The extreme drought years are consistent among the three sample sites. For
347 instance, there was an extreme drought year in 1981 at HL and DS sample sites; it was
348 also a drought year at CL. An extreme drought year at CL in 1957 was also a drought
349 year for the other two chronologies. Moreover, the extreme drought year of 1928 at DS
350 was a drought year at the other two sites. Drought years in 1926, 1947, 2001, and 2011
351 were seen in all three sites and in two of the three sample sites (1916, 1966, 1982, and
352 2000 at HL and CL; 1854 and 1861 at HL and DS) (Fig. 32).

353

354 3.3.2 Characteristics of regional climate change at inter-decadal scales

355 On the decadal scale, the 11a running mean series indicates that at the HL site there
356 were four wetter periods (mid-1860s to early 1880s; 1910s to 1920s; mid-1930s to mid-
357 1970s; and late 1990s to early 2010s). Four drought periods were seen (mid-1850s to
358 mid-1860s; early 1890s to late 1900s; circa 1930s; and mid-1970s to 1980s) (Fig. 54).



359

360 [Figure 54](#). Three regional chronologies demonstrating alternation between dry (red) and wet (blue)
 361 years on interdecadal scales (11 a running mean). The gray and light gray bands indicate consistent
 362 changes of the dry and wet periods.

363

364 The CL regional chronology revealed two main wetter periods (mid-1850s to mid-
 365 1870s; mid-1930s to mid-1970s) and two longer drought periods (late 1870s to early
 366 1930s; following the late 1970s) ([Fig. 54](#)).

367 The DS regional chronology showed four main wetter periods (mid-1840s to mid-
 368 1870s; mid-1880s to late 1900s; mid-1930s to mid-1980s; and late 2000s to early
 369 2010s). There were four drought periods (mid-1820s to mid-1840s; mid-1870s to 1880s;
 370 early 1910s to early 1930s; and late 1980s to mid-2000s). The drought during the last
 371 drought period was less severe ([Fig. 54](#)).

372 The three chronologies show both synchronized phases and differential changes on
 373 an interdecadal scale. The more synchronized dry phases of climate change were the
 374 drought periods of the 1930s and 1990s. When we compared the DS chronology to the
 375 HL and CL chronologies on decadal scales, we noted that DS droughts tended to last

376 longer and that they started and ended later than CL droughts. However, HL and DS
377 droughts tended to end at the same time (Fig.54).

378 There were two wet periods in 1870s and the mid-1930s to 1970s which were
379 shared by all three sample sites. The latter period was the longest lasting wet period we
380 saw in our study. There were also dry and wet periods that were not shared by any of
381 our sites. There was an HL drought (mid-1850s to mid-1860s) which was not shared by
382 the other two sites, which were wetter. HL and CL shared drought periods (1890s to
383 1910s; 1980s) while DS was wetter. Conversely wetter periods at HL were sometimes
384 accompanied by drought in the other two sites. Drought at CL was sometimes
385 accompanied by wet periods at the other two sites. DS was wet during the 2010s but
386 the other two sites were in drought (Fig.54).

387 The results of the above studies show that there are diversified and complex
388 features in the interdecadal processes of climate change in different regions around the
389 Alxa Plateau.

391 **3.4 Driving mechanism of the regional climate changes**

392 **3.4.1 Driving mechanism of the regional climate changes of typical years**

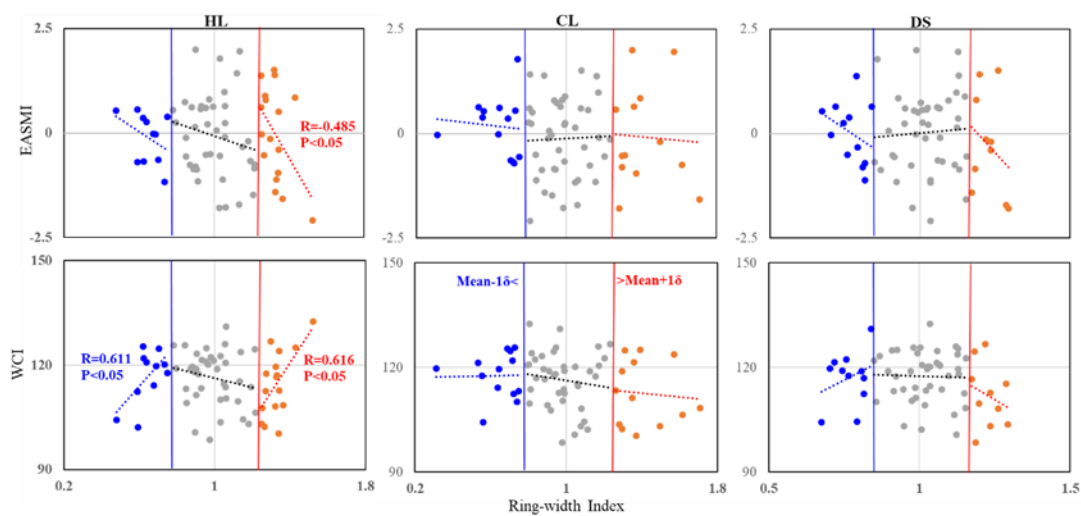
393 On the interannual scales, three regional chronologies we developed showed fairly
394 weak negative correlations between the EASM and the westerlies; none of the
395 correlations were statistically significant. We carried out correlation analyses of the
396 three regional ring-width chronologies and two major circulation indices. This was
397 done in high, medium and low ring-width index groups (Fig. 5; 6; 7).

398 At HL, the results of our combined subgroup correlation analyses suggest that
399 correlations between radial growth groups and atmospheric circulations were stable.
400 Correlation between the higher ring-width group and atmosphere circulation indices
401 and between the lower ring-width group and the WCI were all significant ($P < 0.05$)
402 (Fig. 5; 6; 7).

403 At CL, correlations between the higher and middle ring-width groups to the WCI
404 and the higher and middle WCI groups to the ring-width index were all negative.
405 Correlations between the higher and middle ring-width groups and the EASMI, and

406 between the higher and middle EASMI groups with the ring-width index were
 407 inconsistent (Fig. 5; 6; 7).

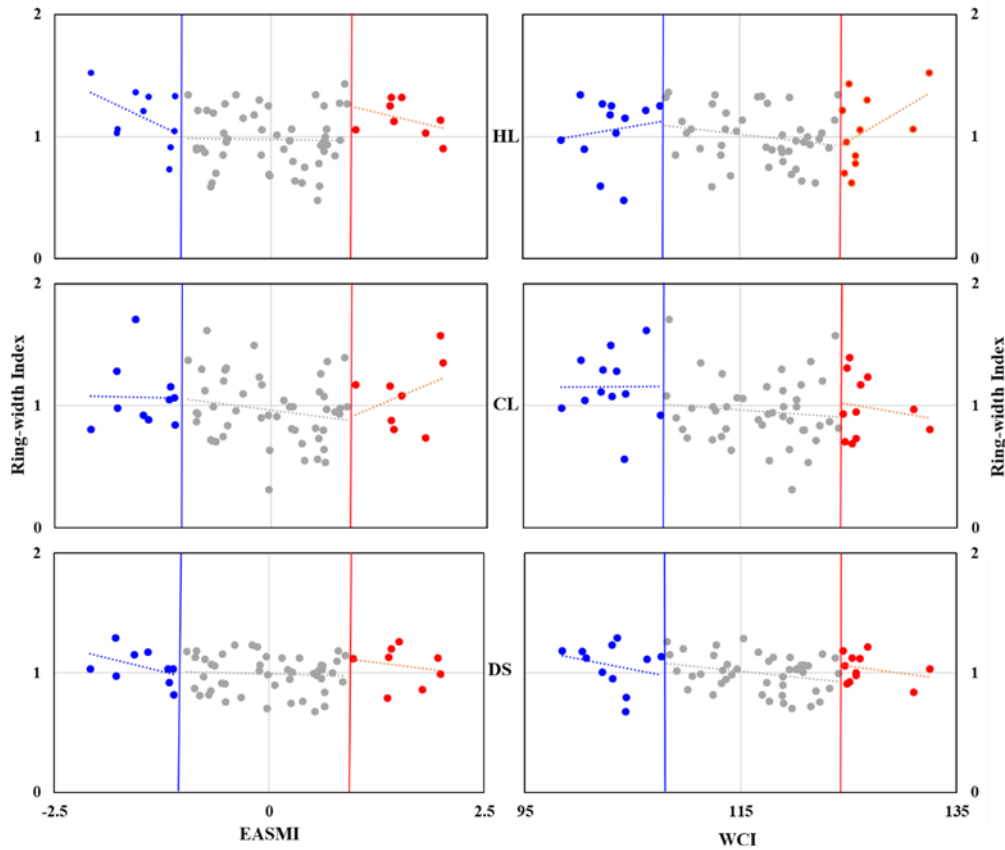
408 At DS, correlations between the higher and lower ring-width groups and the
 409 EASMI, and between the higher and lower EASMI groups to the ring-width indices,
 410 were consistent. The correlations between the higher ring-width groups and the WCI,
 411 and between the higher WCI groups and the ring-width index were consistent. However,
 412 the correlations between the lower ring-width groups and the WCI, also between the
 413 lower WCI groups and the ring-width index, were inconsistent (Fig. 5; 6; 7).



414
 415 **Figure 65.** Grouping related charts among the ring-width index of three regions (HL, CL and
 416 DS) and the two atmospheric circulations' indices (EASMI and WCI), grouped by chronological
 417 values. The noted numbers are the person correlation coefficients (two-tails test) and the
 418 corresponding significant credible level. Only the significant correlations were labeled. Red dots
 419 indicate the higher ring-width index group ($> \text{mean}+1\delta$), gray dots indicate the middle ring-width
 420 index group ($> \text{mean}-1\delta \sim < \text{mean}+1\delta$), and blue dots indicate the lower ring-width index group ($<$
 421 $\text{mean}-1\delta$).

422
 423 Except for HL, none of the ring-width groups or the atmospheric circulation index
 424 groups of the others reached a level of significance. These results suggest that HL is
 425 strongly affected by size of, and the interaction between, the EASM and the Westerly
 426 winds. On an interannual scale, stronger west winds and a weaker monsoon could result
 427 in variations from the ordinary climate (veering towards drier or wetter). Weaker west

428 winds and a stronger monsoon formed the normal climate at HL. At the CL and DS
 429 sites, both atmospheric circulations were relatively weak on interannual scales. They
 430 had complex interactions.



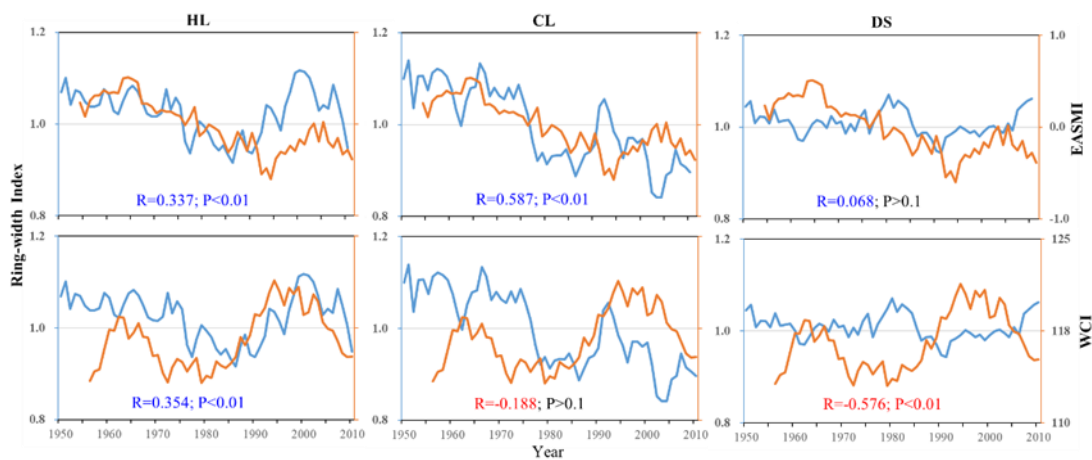
431
 432 **Figure 76.** Grouping related charts among the two atmosphere circulations' index (EASMI and WCI)
 433 and the ring-width index of three regions (HL, CL, and DS), grouped by the two atmosphere
 434 circulations' index. Red dots indicate the higher atmosphere circulations' index group ($> \text{mean} + 1\delta$),
 435 gray dots indicate the middle atmosphere circulations' index group ($> \text{mean} - 1\delta \sim < \text{mean} + 1\delta$), and
 436 blue dots indicate the lower atmosphere circulations' index group ($> \text{mean} - 1\delta$).

437

438 **3.4.2 Driving mechanisms of the regional climate changes on a decadal scale**

439 At HL, both the EASM and the westerly circulation had highly significant effects on
 440 the radial growth of the Qinghai spruce. At CL, the EASM also had highly significant
 441 effects on radial growth of the Qinghai spruce. There, correlation coefficients were
 442 higher for the EASMI (EASM index) than they were for the HL index. Correlations
 443 between the WCI and radial growth were negative, but not at a significant level.

444 At DS, correlation between radial growth and the WCI was extremely negative (P
 445 < 0.01). Correlation between radial growth and the EASM was positive ($P > 0.1$) (Fig.
 446 [87](#)). These results suggest that at HL, alternations between dry and wet seasons were
 447 affected both by the EASM and the westerlies. If either of the two atmospheric
 448 circulations was stronger, the climate tended to be wetter. At CL, alternations between
 449 dry and wet were affected mainly by the EASM. When the EASM was stronger, the
 450 climate was wetter. At DS, the climate was affected mainly by the westerlies. The
 451 stronger the winds, the wetter the climate (Fig. [87](#)).



452

453 [Figure 87](#). Interdecadal scale (11-a running average) correlations of the three residual chronologies
 454 with the EASMI and WCI.

455

456 The results of our interdecadal partial correlation analysis of the three RES-
 457 chronologies with the WCI and EASMI further illustrate the impacts of the two
 458 circulation systems on the climate of the three regions (Table 2).

459 At HL, if we control one variable (the WCI or EASMI) from our analysis, the other
 460 variable will all showed a positive correlation with its chronology ($P < 0.0001$). At CL,
 461 if we controlled the WCI, we find a positive significant correction between the
 462 chronology and EASMI ($P < 0.0001$). If we controlled the effect of EASMI, we saw a
 463 weak negative correction between the chronology and WCI (Table 2). At DS, if we
 464 controlled EASMI, we saw a negative significant correlation between the chronology
 465 and WCI ($P < 0.0001$). If we controlled the WCI, we saw an insignificant negative
 466 correlation between the chronology and EASMI (Table 2).

467 Table 2. Inter-decadal partial correlation analysis of the three residual-chronologies
 468 with the WCI and EASMI.

	HL	CL	DS
WCI	0.489 ***	0.550***	-0.172
EASMI	0.511***	-0.001	-0.591***

469 Correlation significance levels (two-tailed test): *** P < 0.001.

470 Summary: at HL (on the eastern boundary of the Alxa Plateau), both EASMI and
 471 WCI influenced the alternation between wet and dry; at CL (on the southern boundary
 472 of the Alxa Plateau), climate was mainly influenced by the EASM. At DS (on the
 473 western boundary of the Alxa Plateau and the middle part of Hexi Corridor), climate
 474 was mainly influenced by the westerlies.

475

476 **4. Discussion and conclusions**

477 **4.1 Climate changes indicated by regional chronologies**

478 Our chronology-climate response analysis (Fig. 43) showed that the radial growth index
 479 of Qinghai spruce in the HL, CL and DS mountains were a good record of regional
 480 climate changes around the Alxa Plateau (Fig. 32). On the interannual scale, the three
 481 regional chronologies noted that the extreme drought years of 1928, 1957 and 1981
 482 were shared by two or more locations, as were the drought years of 1854, 1861, 1916,
 483 1926, 1947, 1966, and 2001 (Fig. 32).

484 We note that drought was also reported by other tree-ring studies for these regions
 485 (Chen et al., 2016), also for the Qilian Mountains (Zhang et al., 2011; Zhang et al.,
 486 2017). Several other drought years (1854, 1884, and 1925–1928) were also seen in the
 487 dry-wet climate history (PDSI and recorded by tree-ring-widths) in the nearby area of
 488 Mount Hasi, which lies on the edge of the regions most influenced by the EASM (Kang
 489 et al., 2012).

490 The drought years of 1823, 1833, 1854, 1877, 1883–1885, 1895, 1908, 1971, 1992,
 491 and 2003 seen in results for the Alxa Plateau are also seen in twelve tree-ring
 492 reconstructed drought series for the Qilian Mountains (an area mainly influenced by
 493 westerlies) (Zhang et al., 2011). We also note that wetter years seen in our three regional

494 chronologies were also seen in results from the Hasi and Xinglong Mountains, which
495 are also on the edge of the area influenced by the EASM) (Fang et al., 2009; Kang et
496 al., 2012).

497 If we compare our results with those seen for the EASM-affected areas at Mount
498 Guiqing, 1820–2005 (Fang et al., 2010), we noted that only three of the eight drought
499 years in that area (1928, 2000, and 2001) were seen in our three chronologies. We also
500 noted results from the westerly-influenced area at Mount Tianshan (Jiang et al., 2017).
501 The wetter years of 1846, 1903 and 1942 at DS were also extreme wet years at Mount
502 Tianshan. Two wet years, 1848 and 1959, recorded at DS are either one year earlier or
503 one year later than extremely wet years at Mount Tianshan, which might suggest some
504 correlation. Drier years at DS (1884, 1947 and 1951) are one or two years later than the
505 extremely dry years at Mount Tianshan. This suggests that these phenomena could be
506 related to broader changes in the extent and strength of the atmospheric circulation.

507 On a broader (interdecadal) scale, an extreme drought period in 1920s–1930s was
508 shared by much of northern China (Liang et al., 2006; Fang et al., 2009; Fang et al.,
509 2010). This is the same drought that we note our chronologies for HL, CL and DS (Liu
510 et al., 2002; Chen et al., 2010; Fan et al., 2012; Liu et al., 2013; Zhang et al., 2015). A
511 drought in 1890–1900 was noted by dendrochronological studies and regional history
512 documents (Yuan, 1994; Ma et al., 2003; Cai and Liu, 2007).

513 Ma and Fu's (2006) study showed a broad shift towards a drying climate in 1977–
514 78 (eastern area in northwestern China, also northern China). Several other
515 dendrochronological studies showed a combination of high temperatures and low
516 precipitation in the late 1970s to early 1990s (Zhang et al., 2005b; Cai and Liu, 2007;
517 Cai, 2009). This same drought was seen at DS, if somewhat later and for a shorter time.
518 We also noted its effects at HL and CL. This would be consistent with the increased
519 humidity of the climate in the eastern region of Northwest China (the EASM-influenced
520 region experiencing > 400 mm precipitation). This region would include Mount
521 Xinglong (Fang et al., 2009; Chen et al. 2015), the easternmost part of the Qilian
522 Mountains, and Mount Guiqing (Fang et al., 2010).

523 The wet period that lasted from the 1940s to the early 1970s has been recorded by
524 several tree-ring-width chronologies covering HL, CL, and DS (Liu et al., 2004; Liu et
525 al., 2005; Gao et al., 2006; Cai, 2009; Chen et al., 2010). Regional history documents
526 also record some severe floods disasters in this period (Yuan, 1994). We also see this
527 wet period in tree-ring-width chronologies from Mount Xinglong (Fang et al., 2009;
528 Chen et al. 2015) and Mount Guiqing (Fang et al., 2010).

529 The wet period in the 1830s–1840s evident in the chronologies in Xinglong
530 Mountain (Fang et al., 2009) (Chen et al. 2015) and Guiqing Mountain (Fang et al.,
531 2010) corresponds to the dry period of DS. The wet period in the 1830s–1840s
532 corresponds to the dry period of HL and CL, and to the wet period of DS. The observed
533 phenomena can be attributed to differences in the extent and intensity of EASM and
534 westerly atmospheric circulations.

535

536 **4.2 Influence of atmospheric circulations and their interaction on climate change** 537 **in the Alxa Plateau**

538 Water vapor carried by the westerlies will extend southward to the northern part of
539 Qinghai, the Hexi region of Gansu, the northern part of Ningxia, and the northern part
540 of Shaanxi Province, sometimes passing through the northern border of the Xinjiang
541 region (Li et al., 2012). The area bounded by 35° and 55°N, and 110°E and 140°E seems
542 to be crucial to fluctuations in the westerlies. This in turn affects the distribution of rain
543 belts in summer. Its mean WCI are weaker positively to the rainfall in the middle of
544 Yellow River Basin and its northern regions (Yan et al., 2007). The results showed that
545 the middle ring-width index group of Qinghai spruce in the three sample sites, which
546 are located in the key area for interaction between wind and monsoon, presented weaker
547 negative correlation with WCI on the interannual scale (Fig. 65).

548 The EASM boundary zone has a greater influence on precipitation at higher
549 latitudes and thus on vegetation growth. This boundary zone can fluctuate due to the
550 interannual variability of the EASM and the westerlies. There may be lagging effects
551 at the mid-latitudes (Ou and Qian, 2006). Again, we note that on an interannual scale,

552 there is much variation in the strengths and interactions of the EASM and westerly
553 circulation and thus on climate in our three study regions (Fig. 65).

554 Sun et al. (2019) showed that when the westerly circulation strengthens, high
555 latitude air pressure drops across the entire Asian continent. Siberian high pressures and
556 the EASM are weakened. The ~~south~~southward movement of the cold air ~~activity~~ is also
557 correspondingly weakened. That is not conducive to the north and south of the cold and
558 warm air vapor exchange to form precipitation. When the lower of the WCI and
559 weakened latitudinal circulation, the meridional circulation will strengthen, which
560 favors the exchange of warm and cold air between the north and south to form
561 precipitation.

562 Yang et al. (2019) proposed that in years with weak summer westerlies in the
563 middle latitudes, the upper-level jet stream tends to shift southward. This southward
564 displacement of the jet stream, coupled with weakened lower-level divergence, hampers
565 the northward transport of warm air into the southwestern region. Consequently, this
566 leads to reduced availability of water vapor sources and ultimately results in diminished
567 summer precipitation within the transitional zone of typical monsoon activity. If the jet
568 stream moves northward, precipitation increases.

569 Xu et al. (2010) ~~wrote~~indicated that in the middle Qilian Mountains the westerlies
570 affect precipitation directly, while the EASM only indirectly affects precipitation. When
571 the westerlies ~~are~~become stronger, ~~(weaker)~~, the high precipitation zone moves
572 northwestward; ~~when they are weaker, the zone moves~~ ~~(southeastward)~~.

573 At DS, radial growth showed weak negative correlations with higher WCI and also
574 higher, middle, and lower EASMI groups (Figs. 5; 6; 7). At HL, when high chronology
575 indices are positive they are significantly correlated with westerly circulation; when
576 they are negative they significantly correlate with EASM (Figs. 5; 6; 7). At CL, which
577 lies further to the south than HL, a higher EASMI leads to a more humid climate. Other
578 effects are more complicated: for example, the higher and lower ring-width index
579 groups, associated with extreme dry and wet climate years, have weak negative
580 correlations to EASMI (Figs. 5; 6; 7). Jiang et al. (2019) published the results of their
581 hydrogen and oxygen isotope studies of surface water at more than 3,000 sampling sites

582 in northern China. They showed that surface water recharge in the DS Mountains is due
583 to the westerlies; recharge in the CL Mountains is due to the EASM. The HL Mountains,
584 in contrast, sit at the boundary of the EASM; water recharge there is due to both the
585 EASM and the westerlies.

586 Jiang and Wang (2005) notes significant declines in the EASM in the mid-1960s
587 and mid-1970s, which led to decline in the radial growth of Qinghai spruce in our study
588 area. The effect of the latter declined period was much greater than that of the former,
589 whatever the intensity or duration. The effects of these declines were stronger at CL
590 and DS than at HL. In the mid-1970s, EASM retreat had stronger negative effects at
591 CL and then at HL. However, decline in the EASM proved to be a facilitator of radial
592 growth at DS (Fig. 87).

593 In the same period the westerly circulation also retreated. The EASM retreated
594 again in 1990s, while the westerlies strengthened. This resulted in a drier climate in the
595 CL Mountains. However, it was also correlated with fluctuating wet periods at HL and
596 a weak wet period at DS. The above results, to a certain extent, support our view on the
597 driving mechanisms of climate change in the three study areas, especially in the DS
598 Mountains.

599 When we look at this area on a geologic scale, we learn that the westerly circulation
600 strengthened during the Ice Age. Westerly jet streams moved southward to about 35°N.
601 When the westerlies weakened in the Interglacial Age, the westerly jet streams moved
602 northward to ~37°N (Sun et al., 2003). A study of Holocene lake level evolution in the
603 ancient Zhuye lake, central Alxa Plateau, showed that lake-level change was subject to
604 the combined effects of EASM and the arid climate of Central Asia (Li, 2009). This
605 result further illustrates the complexity of lake evolution and climate change in the
606 EASM marginal zone.

607 The westerly circulation also interacts with the monsoon on the Tibetan Plateau,
608 which has a profound effect on the climate of the Asian monsoon region as well as the
609 global climate (Qu et al., 2004). There has also been much research using proxy
610 indicator cycles indicating that our study area is also influenced by large-scale ~~climate~~
611 ~~and~~ ocean-atmosphere changes on interannual and interdecadal scales, such as the

612 North Atlantic Oscillation (NAO), Pacific Decadal Oscillation (PDO), El Niño-
613 Southern Oscillation (ENSO), and sunspot activity (Gou et al., 2015a; 2015b; Liu et al.,
614 2016; Wang et al., 2017). Generally, the intensity of ENSO was inversely correlated
615 with the intensity of the EASM. There was a negative correlation between PDO and
616 regional dry-wet variation in the west of 100° E. When the NAO is in positive phase
617 (negative phase), it indicates that the mid-latitude westerly winds are in strong
618 (declining) phase, which is conducive to (unfavorable) precipitation formation.

619 However, all of the above-mentioned large-scale climate and ocean-atmosphere
620 changes affect the EASM and westerly circulation through different pathways (Li.
621 2009), which in turn have various effects on the northwestern edge zone of the EASM
622 and the zone of interaction between the two major atmospheric circulations.

623 In conclusion, based on the analysis of the regional chronologies collected in the
624 HL, CL and DS mountains that are arrayed around the Alxa Plateau, we can safely assert
625 that the radial growth of Qinghai spruce in the study area is mainly affected by regional
626 precipitation. This precipitation varies constantly over time and space, primarily
627 influenced by the interactions between two atmospheric circulation systems, EASM
628 and westerlies. At HL, both of these atmospheric circulation systems play a significant
629 role in shaping climate changes. At CL, the climate is mainly influenced by the EASM.
630 At DS, climate is more heavily influenced by the westerly circulation.

631 In the future, it is to be hoped that more refined, smaller scale research can be done
632 on the climate history in the deserts of the Alxa Plateau. Such research may finally to
633 provide a theoretical basis to explain regional climate driving mechanisms and thus
634 enable better desertification controls.

635

636 **Acknowledgements**

637 The study was jointly funded by the National Natural Science Foundation of China
638 (NSFC) (No.42171031; 42171167); Inner Mongolia Autonomous Region Special Fund
639 project for transformation of Scientific and technological Achievements (2021CG0046).

640

641

642 **References**

- 643 Cai, Q. F.: Response of *Pinus tabulaeformis* tree-ring growth to three moisture indices and
644 January to July Walter index reconstruction in Helan mountain, Marine geology &
645 Quaternary geology, 29, 131–136 (In Chinese with English abstract),
646 <https://doi.org/10.3724/SP.J.1140.2009.06131>, 2009.
- 647 Cai, Q. F. and Liu, Y.: January to August temperature variability since 1776 inferred from tree-
648 ring width of *Pinus tabulaeformis* in Helan Mountain, Journal of Geographical Sciences,
649 17, 293–303, <https://doi.org/10.1007/s11442-007-0293-5>, 2007.
- 650 Chen, F., Yuan, Y. J., Zhang, T. W., and Linderholm, H. W.: Annual precipitation variation for
651 the southern edge of the Gobi Desert (China) inferred from tree rings: linkages to climatic
652 warming of twentieth century, Nat. Hazards, 81, 939–955, [https://doi.org/10.1007/s11069-](https://doi.org/10.1007/s11069-015-2113-z)
653 015-2113-z, 2016.
- 654 Chen, F., Wei, W. S., Yuan, Y. J., Yu, S. L., Shang, H. M., Zhang, T. W., Zhang, R. B., Wang, H.
655 Q., and Qin, L.: Variation of annual precipitation during 1768–2006 in Gansu Inferred from
656 multi-site tree-ring chronologies, Journal of Desert Research, 33, 1520–1526 (In Chinese
657 with English abstract), <https://doi.org/10.7522/j.issn.1000-694X.2013.00218>., 2013.
- 658 Chen, F., Yuan, Y. J., Wei, W. S., Yu, S. L., Fan, Z. A., Zhang, R. B., Zhang, T. W., Li, Q., and
659 Shang, H. M.: Temperature reconstruction from tree-ring maximum latewood density of
660 Qinghai spruce in middle Hexi Corridor, China, Theoretical and Applied Climatology, 107,
661 633–643, <https://doi.org/10.1007/s00704-011-0512-y>, 2012.
- 662 Chen, F., Yuan, Y. J., Wei, W. S., Yu, S. L., Li, Y., Zhang, R., Fan, Z., Zhang, T., and Shang, H.:
663 PDSI changes of May to July recorded by tree rings in the northern Helan Mountains,
664 Advance in Climate Changes Research, 65, 344–348 (In Chinese with English abstract),
665 2010.
- 666 Chen, F. H., Chen, J. H., Huang, W., Chen, S. Q., Huang, X. Z., Jin, L. Y., Jia, J., Zhang, X. J.,
667 An, C., and Zhang, J.: Westerlies Asia and monsoonal Asia: spatiotemporal differences in
668 climate change and possible mechanisms on decadal to sub-orbital timescales, Earth-Sci.
669 Rev., 192, 337–354, <https://doi.org/10.1016/j.earscirev.2019.03.005>, 2019a.
- 670 Chen, F. H., Fu, B. J., Xia, J., Wu, D., Wu, S. H., Zhang, Y. L., Sun, H., Liu, Y., Fang, X. M.,
671 Qin, B. Q., Li, X., Zhang, T. J., Liu, B. Y., Dong, Z. B., Hou, S. G., Tian, L. D., Xu, B. Q.,
672 Dong, G. H., Zheng, J. Y., Yang, W., Wang, X., Li, Z. J., Wang, F., Hu, Z. B., Wang, J.,
673 Liu, J. B., Chen, J. H., Huang, W., Hou, J. Z., Cai, Q. F., Long, H., Jiang, M., Hu, Y. X.,
674 Feng, X. M., Mo, X. G., Yang, X. Y., Zhang, D. J., Wang, X. H., Yin, Y. H., and Liu, X.
675 C.: Major advances in studies of the physical geography and living environment of China
676 during the past 70 years and future prospects, Science China Earth Sciences, 62, 1665–
677 1701, <https://doi.org/10.1007/s11430-019-9522-7>, 2019b.
- 678 Chen, J., Huang, W., Jin, L., Chen, J. H., Chen, S. Q., and Chen, F. H.: A climatological northern
679 boundary index for the East Asian summer monsoon and its interannual variability,
680 Science China Earth Sciences, 61, 13–22, <https://doi.org/10.1007/s11430-017-9122-x>,

681 2018.

682 Cook E.R.: A Time Series Analysis approach to tree ring standardization (Dendrochronology,
683 forestry, dendroclimatology, autoregressive process)[D]. Tuscon, Arizona: The University
684 of Arizona, 1985.

685 Ding, Y. H., Liu, Y. J., Xu, Y., Wu, P., Xue, T., Wang, J., Shi, Y., Zhang, Y. X., Song, Y. F., and
686 Wang, P. L.: Regional responses to global climate change: progress and prospects for trend,
687 causes, and projection of climatic warming-wetting in Northwest China, *Advances in*
688 *Earth Science*, 38, 551–562 (In Chinese with English abstract),
689 <https://doi.org/10.11867/j.issn.1001-8166.2023.027>, 2023.

690 Fan, Z. A., Wei, W. S., Chen, F., and Yuan, Y. J.: Precipitation variation from 1775 to 2005 at
691 the eastern margin of Tengger Desert, China inferred from tree-ring, *Journal of Desert*
692 *Research*, 32, 996–1002 (In Chinese with English abstract), 2012.

693 Fang, K. Y., Gou, X. H., Chen, F. H., D'arrigo, R., and Li, J. B.: Tree-ring based drought
694 reconstruction for the Guiqing Mountain (China): linkages to the Indian and Pacific
695 Oceans, *Int. J. Climatol.*, 30, 1137–1145, <https://doi.org/10.1002/joc.1974>, 2010.

696 Fang, K. Y., Gou, X. H., Chen, F. H., Yang, M. X., Li, J. B., He, M. S., Zhang, Y., Tian, Q. H.,
697 and Peng, J. F.: Drought variations in the eastern part of northwest China over the past two
698 centuries: evidence from tree rings, *Clim. Res.*, 38, 129–135,
699 <https://doi.org/10.3354/cr00781>, 2009.

700 Feng, W., Wang, K. L., and Jiang, H.: Influences of westerly wind inter-annual change on water
701 vapor transport over northwest china summer, *Plateau Meteorology*, 23, 270–275 (In
702 Chinese with English abstract), 2004.

703 Gao, S. Y., Lu, R. J., Qiang, M. R., Ha, S., Zhang, D. S., Chen, Y., and Xia, H.: Precipitation
704 variation recorded by tree-rings in the northern Tengger Desert of the last 140 years, *Chin.*
705 *Sci. Bull.*, 51, 326–331, <https://doi.org/10.1360/csb2006-51-3-326>, 2006.

706 Gou, X. H., Gao, L. L., Deng, Y., Chen, F. H., Yang, M. X., and Still, C.: An 850 - year tree -
707 ring - based reconstruction of drought history in the western Qilian Mountains of
708 northwestern China, *Int. J. Climatol.*, 35, 3308–3319, <https://doi.org/10.1002/joc.4208>,
709 2015a.

710 Gou, X. H., Deng, Y., Gao, L. L., Chen, F. H., Cook, E., Yang, M. M., and Zhang, F.: Millennium
711 tree-ring reconstruction of drought variability in the eastern Qilian Mountains, northwest
712 China, *Climate Dynamics*, 45, 1761–1770, <https://doi.org/10.1007/s00382-014-2431-y>,
713 2015b.

714 Huang, L. X., Chen, J., Yang, K., Yang, Y. J., Huang, W., Zhang, X., and Chen, F. H.: The
715 northern boundary of the Asian summer monsoon and division of westerlies and monsoon
716 regimes over the Tibetan Plateau in present-day, *Science China Earth Sciences*, 66, 882–
717 893, <https://doi.org/10.1007/s11430-022-1086-1>, 2023.

718 Jiang, D. B. and Wang, H. J.: Natural interdecadal weakening of East Asian summer monsoon
719 in the late 20th century, *Chin. Sci. Bull.*, 50, 1923–1929, <https://doi.org/10.1360/982005->

- 720 36, 2005.
- 721 Jiang, P., Liu, H. Y., Wu, X. C., and Wang, H. Y.: Tree-ring-based SPEI reconstruction in central
722 Tianshan Mountains of China since A.D. 1820 and links to westerly circulation, *Int. J.*
723 *Climatol.*, 37, 2863–2872, <https://doi.org/10.1002/joc.4884>, 2017.
- 724 Jiang, W. J., Wang, G. C., Sheng, Y. Z., Shi, Z. M., and Zhang, H.: Isotopes in groundwater (^2H ,
725 ^{18}O , ^{14}C) revealed the climate and groundwater recharge in the Northern China, *Sci. Total*
726 *Environ.*, 666, 298–307, <https://doi.org/10.1016/j.scitotenv.2019.02.245>, 2019.
- 727 Kang, S. Y. and Yang, B.: Precipitation variability at the northern fringe of the Asian summer
728 monsoon in Northern China and its possible mechanism over the past 530 years,
729 *Quaternary Sciences*, 35, 1185–1193, [https://doi.org/10.11928/j.issn.1001-](https://doi.org/10.11928/j.issn.1001-7410.2015.05.14)
730 7410.2015.05.14, 2015.
- 731 Kang, S. Y., Yang, B., and Qin, C.: Recent tree-growth reduction in north central China as a
732 combined result of a weakened monsoon and atmospheric oscillations, *Clim. Change*, 115,
733 519–536, <https://doi.org/10.1007/s10584-012-0440-6>, 2012.
- 734 Li, D. L., Shao, P. C., and Wang, H.: The position variations of the north boundary of East Asia
735 subtropical summer monsoon in 1951–2009, *Journal of Desert Research*, 33, 1511–1519
736 (In Chinese with English abstract), <https://doi.org/10.7522/j.issn.1000-694X.2013.00217>,
737 2013.
- 738 Li, J. L., Li, Z. R., Yang, J. C., Shi, Y. Z., and Fu, J.: Analyses on spatial distribution and
739 temporal variation of atmosphere water vapor over northwest China in summer of later 10
740 years, *Plateau Meteorology*, 31, 1574–1581 (In Chinese with English abstract), 2012.
- 741 Li, J. P. and Zeng, Q. C.: A new monsoon index, its interannual variability and related with
742 monsoon precipitation, *Climatic and Environmental Research*, 10, 351–365 (In Chinese
743 with English abstract), 2005.
- 744 Li, W. L., Wang, K. L., Fu, S. M., and Jiang, H.: The interrelationship between regional Westerly
745 index and the water vapor budget in Northwest China, *Journal of Glaciology and*
746 *Geocryology*, 30, 28–34 (In Chinese with English abstract), 2008.
- 747 Li, Y.: The pollen records from lake sediments and climate & lake model in the Marginal area
748 of Asian monsoon, Lanzhou University, Lanzhou, China, 2009.
- 749 Li, Z. X., Feng, Q., Song, Y., Wang, Q. J., Yang, J., Li, Y. G., Li, J. G., and Guo, X. Y.: Stable
750 isotope composition of precipitation in the south and north slopes of Wushaoling Mountain,
751 northwestern China, *Atmospheric Research*, 182, 87–101,
752 <https://doi.org/10.1016/j.atmosres.2016.07.023>, 2016.
- 753 Liang, E. Y., Liu, X. H., Yuan, Y. J., Qin, N. S., Fang, X. Q., Huang, L., Zhu, H. F., Wang, L.,
754 and Shao, X. M.: The 1920s drought recorded by tree rings and historical documents in
755 the semi-arid and arid areas of Northern China, *Clim. Change*, 79, 403–432,
756 <https://doi.org/10.1007/s10584-006-9082-x>, 2006.
- 757 Liu, J. B., Chen, J., Chen, S. Q., Yan, X. W., Dong, H. R., and Chen, F. H.: Dust storms in

- 758 northern China and their significance for the concept of the Anthropocene, *Science China*
759 *Earth Sciences*, 65, 921–933, <https://doi.org/10.1007/s11430-021-9889-8>, 2022.
- 760 Liu, Y., Cai, Q. F., Ma, L. M., and An, Z. S.: Tree ring precipitation records from Baotou and
761 the East Asia summer monsoon variations for the last 254 years, *Earth Sci. Front.*, 8, 91–
762 97 (In Chinese with English abstract), <https://doi.org/10.3321/j.issn:1005-2321.2001.01.012>, 2001.
- 764 Liu, Y., Sun, C. F., Li, Q., and Cai, Q. F.: A *Picea crassifolia* tree-ring width-based temperature
765 reconstruction for the Mt. Dongda region, Northwest China, and its relationship to large-
766 scale climate forcing, *PLoS One*, 11, e0160963,
767 <https://doi.org/10.1371/journal.pone.0160963>, 2016.
- 768 Liu, Y., Lei, Y., Sun, B., Song, H. M., and Li, Q.: Annual precipitation variability inferred from
769 tree-ring width chronologies in the Changling–Shoulu region, China, during AD 1853–
770 2007, *Dendrochronologia*, 31, 290–296, <https://doi.org/10.1016/j.dendro.2013.02.001>,
771 2013.
- 772 Liu, Y., Won-Kyu, P., Cai, Q. F., Jung-Wook, S., and Hyun-Sook, J.: Monsoonal precipitation
773 variation in the East Asia since A.D. 1840—tree-ring evidences from China and Korea,
774 *Science in China Series D: Earth Sciences*, 46, 1031–1039,
775 <https://doi.org/10.1007/BF02959398>, 2003.
- 776 Liu, Y., Ma, L. M., Cai, Q. F., An, Z. S., Liu, W. G., and Gao, L. Y.: Reconstruction of summer
777 temperature (June–August) at Mt. Helan, China, from tree-ring stable carbon isotope
778 values since AD 1890, *Science in China Series D: Earth Sciences*, 45, 1127–1136,
779 <https://doi.org/10.1360/02yd9109>, 2002.
- 780 Liu, Y., Cai, Q. F., Liu, W. G., Yang, Y. K., Sun, J. Y., Song, H. M., and Li, X. X.: Monsoon
781 precipitation variation recorded by tree-ring $\delta^{18}\text{O}$ in arid Northwest China since AD 1878,
782 *Chemical Geology*, 252, 56–61, <https://doi.org/10.1016/j.chemgeo.2008.01.024>, 2008.
- 783 Liu, Y., Cai, Q. F., Shi, J. F., Hughes, M. K., Kutzbach, J. E., Liu, Z. Y., Ni, F. B., and An, Z. S.:
784 Seasonal precipitation in the south-central Helan Mountain region, China, reconstructed
785 from tree-ring width for the past 224 years, *Canadian Journal of Forest Research*, 35,
786 2403–2412, <https://doi.org/10.1139/x05-168>, 2005.
- 787 Liu, Y., Shi, J. F., Shishov, V., Vaganov, E., Yang, Y. K., Cai, Q. F., Sun, J. Y., Wang, L., and
788 Djanseitov, I.: Reconstruction of May–July precipitation in the north Helan Mountain,
789 Inner Mongolia since A.D. 1726 from tree-ring late-wood widths, *Chin. Sci. Bull.*, 49,
790 405–409, <https://doi.org/10.1007/BF02900325>, 2004.
- 791 Ma, L. M., Liu, Y., Cai, Q. F., and An, Z. S.: The precipitation records from tree-ring late wood
792 width in the helan mountain, *Marine geology & Quaternary geology*, 23, 109–114 (In
793 Chinese with English abstract), <https://doi.org/10.16562/j.cnki.0256-1492.2003.04.016>,
794 2003.
- 795 Ma, M. J., Pu, Z. X., Wang, S. G., and Zhang, Q. A.: Characteristics and numerical simulations
796 of extremely large atmospheric boundary-layer heights over an arid region in north-west

797 china, *Boundary-Layer Meteorology*, 140, 163–176, [https://doi.org/10.1007/s10546-011-](https://doi.org/10.1007/s10546-011-9608-2)
798 9608-2, 2011.

799 Ma, Z. G. and Fu, C. B.: The basic facts of aridity in northern China from 1951 to 2004, *Chin.*
800 *Sci. Bull.*, 51, 2429–2439 (In Chinese), <https://doi.org/10.1360/csb2006-51-20-2429>,
801 2006.

802 Ou, T. H. and Qian, W. H.: Vegetation variations along the monsoon boundary zone in East
803 Asia, *Chinese Journal of Geophysics*, 49, 698–705 (In Chinese with English abstract),
804 2006.

805 Qin, L., Liu, G. X., Li, X. Z., Chongyi, E., Li, J., Wu, C. R., Guan, X., and Wang, Y.: A 1000-
806 year hydroclimate record from the Asian summer monsoon-Westerlies transition zone in
807 the northeastern Qinghai-Tibetan Plateau, *Clim. Change*, 176, 1–20, [https://doi.org](https://doi.org/10.1007/s10584-023-03497-1)
808 [/10.1007/s10584-023-03497-1](https://doi.org/10.1007/s10584-023-03497-1), 2023.

809 Qu, W. J., Zhang, X. H., Wang, D., Shen, Z. X., Mei, F. M., Cheng, Y., and Yan, L. W.: The
810 important significance of westerly wind study, *Marine Geology and Quaternary Geology*,
811 24, 125–132 (In Chinese with English abstract), [https://doi.org/10.16562/j.cnki.0256-](https://doi.org/10.16562/j.cnki.0256-1492.2004.01.018)
812 1492.2004.01.018, 2004.

813 Shao, X. M., Xu, Y., Yin, Z. Y., Liang, E. Y., Zhu, H. F., and Wang, S.: Climatic implications of
814 a 3585-year tree-ring width chronology from the northeastern Qinghai-Tibetan Plateau,
815 *Quaternary Science Reviews*, 29, 2111–2122,
816 <https://doi.org/10.1016/j.quascirev.2010.05.005>, 2010.

817 Sun, D. H., An, Z. S., Su, R. H., Deer, H. Y., and Sun, Y. B.: The dust deposition records of the
818 evaluation of Asia monsoon and Westerly circulation in north China in the last 2.6Ma,
819 *Science in China (Series D)*, 33, 497–504 (In Chinese), 2003.

820 Sun, L. Q., Li, T. J., Li, Q. L., and Wu, Y. P.: Responses of autumn flood peak in the Yellow
821 River source regions to westerly circulation index, *Journal of Glaciology and Geocryology*,
822 41, 1475–1482 (In Chinese with English abstract), [https://doi.org/10.7522/j.issn.1000-](https://doi.org/10.7522/j.issn.1000-0240.2019.0028)
823 0240.2019.0028, 2019.

824 Tang, X., Qian, W. H., and Liang, P.: Climatic features of boundary belt for East Asian Summer
825 Monsoon, *Plateau Meteorology*, 25, 375–381 (In Chinese with English abstract), 2006.

826 Vicente-Serrano, S.M., Beguería, S. and López-Moreno, J.I.: A multiscalar drought index
827 sensitive to global warming: the standardized precipitation evapotranspiration index. *J.*
828 *Clim.*, 23(7): 1696–1718, <https://doi.org/10.1175/2009jcli2909.1.>, 2010.

829 Wang, B. J., Huang, Y. X., He, J. H., and Wang, L. J.: Relation between vapour transportation
830 in the period of East Asian Summer Monsoon and drought in Northwest China. *Plateau*
831 *Meteorology*, 23, 912–917 (In Chinese with English abstract), 2004.

832 Wang, J. L., Yang, B., Ljungqvist, F. C., Luterbacher, J., Osborn, Timothy j., Briffa, K. R., and
833 Zorita, E.: Internal and external forcing of multidecadal Atlantic climate variability over
834 the past 1,200 years, *Nature Geoscience*, 10, 512–517, <https://doi.org/10.1038/ngeo2962>,
835 2017.

- 836 Wang, K. L., Jiang, H., and Zhao, H. Y.: Atmospheric water vapor transport from westerly and
 837 monsoon over the Northwest China, *Advances in Water Science*, 16, 432–438 (In Chinese
 838 with English abstract), <https://doi.org/10.14042/j.cnki.32.1309.2005.03.021>, 2005.
- 839 Wigley, T.M.L., Briffa, K.R., Jones, P.D. On the average value of correlated time series, with
 840 applications in dendroclimatology and hydrometeorology. *Journal of Climate and Applied*
 841 *Meteorology* 23(2), 201–213, 1984.
- 842 Xiao, S. C., Chen, X. H., and Ding, A. J.: Study process of climate changes, environment
 843 evolution and its driving mechanism in the last two centuries in the Alxa Desert, *Journal*
 844 *of Desert Research*, 37, 1102–1201 (In Chinese with English abstract),
 845 [10.7522/j.issn.1000-694x.2017.00002](https://doi.org/10.7522/j.issn.1000-694x.2017.00002), 2017.
- 846 Xiao, S. C., Yan, C. Z., Tian, Y. Z., Si, J. H., Ding, A. J., Chen, X. H., Han, C., and Teng, Z. Y.:
 847 Regionalization for desertification control and countermeasures in the Alxa Plateau, China,
 848 *Journal of Desert Research*, 39, 182–192 (In Chinese with English abstract),
 849 <https://doi.org/10.7522/j.issn.1000-694X.2019.00068>, 2019.
- 850 Xu, J. J., Wang, K. L., Jiang, H., Li, Z. G., Sun, J., Luo, X. P., and Zhu, Q. L.: A numerical
 851 simulation of the effects of Westerly and Monsoon on precipitation in the Heihe River
 852 Basin, *Journal of Glaciology and Geocryology*, 32, 489–496 (In Chinese with English
 853 abstract), 2010.
- 854 Yan, H. S., Hu, J., Fan, K., and Zhang, Y. J.: The analysis of relationship between the variations
 855 of Westerly Index in summer and precipitation during the flood period over China in the
 856 last 50 years. , *Chinese Journal of Atmospheric Science*, 31, 717–726 (In Chinese with
 857 English abstract), 2007.
- 858 Yang, B., Qin, C., Wang, J. L., He, M. H., Melvin, T. M., Osborn, T. J., and Briffa, K. R.: A
 859 3,500-year tree-ring record of annual precipitation on the northeastern Tibetan Plateau,
 860 *Proc. Natl. Acad. Sci. USA*, 111, 2903–2908, <https://doi.org/10.1073/pnas.1319238111>,
 861 2014.
- 862 Yang, J. H., Zhang, Q., Liu, X. Y., Yue, P., Shang, J. L., Ling, H., and Li, W. J.: Spatial-temporal
 863 characteristics and causes of summer precipitation anomalies in the transitional zone of
 864 typical summer monsoon, China, *Chinese Journal of Geophysics*, 62, 4120–4128 (In
 865 Chinese with English abstract), <https://doi.org/10.6038/cjg2019M0639>, 2019.
- 866 Yuan, L.: *Hazards history in northwestern China*, Gansu people's press, Lanzhou, China 1994.
- 867 Zhang, F., Chen, Q. M., Su, J. J., Deng, Y., Gao, L. L., and Gou, X. H.: Tree-ring recorded of
 868 the drought variability in the northwest monsoon marginal, China, *Journal of Glaciology*
 869 *and Geocryology*, 39, 245–251 (In Chinese with English abstract),
 870 <https://doi.org/10.7522/j.issn.1000-0240.2017.0028>, 2017.
- 871 Zhang, Q., Yang, J. H., Wang, P. L., Yu, H. P., Yue, P., Liu, X. Y., Lin, J. J., Duan, X. Y., Zhu,
 872 B., and Yan, X. Y.: Progress and prospect on climate warming and humidification in
 873 Northwest China, *Chin. Sci. Bull.*, 68, 1814–1828, <https://doi.org/10.1360/TB-2022-0643>,
 874 2023.

- 875 Zhang, Q. B., Cheng, G. D., Yao, T. D., Kang, X. C., and Huang, J. G.: A 2,326 year tree-ring
876 record of climate variability on the northeastern Qinghai-Tibetan Plateau, *Geophys. Res.*
877 *Let.*, 30, 1739, <https://doi.org/10.1029/2003GL017425>, 2003.
- 878 Zhang, Q. L., Liu, W. G., Liu, Y., Ning, Y. F., and Wen, Q. B.: Relationship between the stable
879 carbon and oxygen isotopic compositions of tree ring in the Mt. Helan region,
880 Northwestern China, *Geochimica*, 34, 51–56, [https://doi.org/10.19700/j.0379-](https://doi.org/10.19700/j.0379-1726.2005.01.006)
881 1726.2005.01.006, 2005a.
- 882 Zhang, S., Xu, H., Lan, J. H., Goldsmith, Y., Torfstein, A., Zhang, G. L., Zhang, J., Song, Y. P.,
883 Zhou, K. E., Tan, L. C., Xu, S., Xu, X. M., and Enzel, Y.: Dust storms in northern China
884 during the last 500 years, *Science China Earth Sciences*, 64, 813–824,
885 <https://doi.org/10.1007/s11430-020-9730-2>, 2021.
- 886 Zhang, Y., Shao, X. M., Yin, Z. Y., Liang, E. Y., Tian, Q. H., and Xu, Y.: Characteristics of
887 extreme droughts inferred from tree-ring data in the Qilian Mountains, 1700-2005, *Clim.*
888 *Res.*, 50, 141–159, <https://doi.org/10.3354/cr01051>, 2011.
- 889 Zhang, Y. X., Yu, L., and Yin, H.: Annual precipitation reconstruction over last 191 years at the
890 south edge of Badain Jaran Desert based on tree ring width data, *Desert and Oasis*
891 *Meteorology*, 9, 12–16 (In Chinese with English abstract),
892 <https://doi.org/10.3969/j.issn.1002-0799.2015.01.003>, 2015.
- 893 Zhang, Y. X., Gou, X. H., Hu, W. D., Peng, J. F., and Liu, P. X.: The drought events recorded
894 in tree ring width in Helan Mt. over past 100 years, *Acta Ecologica Sinica*, 25, 2121–2126
895 (In Chinese with English abstract), 2005b.
896